High time resolution beam-based measurement of the rf-to-laser jitter in a photocathode rf gun

Zhen Zhang,[1,2] Yingchao Du,[1,2,*] Lixin Yan,[1,2] Qiang Du,[1,2] Jianfei Hua,[1,2] Jiaru Shi,[1,2] Jin Yang,[1,2] Dan Wang,[1,2] Wenhui Huang,[1,2] Huaibi Chen,[1,2] and Chuanxiang Tang[1,2]

[1]*Department of Engineering Physics, Tsinghua University, Beijing 100084, People's Republic of China*

[2]*Key Laboratory of Particle & Radiation Imaging (Tsinghua University), Ministry of Education, Beijing, People's Republic of China*

(Received 7 August 2013; published 24 March 2014)

Characterizing the rf-to-laser jitter in the photocathode rf gun and its possible origins is important for improving the synchronization and beam quality of the linac based on the photocathode rf gun. A new method based on the rf compression effect in the photocathode rf gun is proposed to measure the rf-to-laser jitter in the gun. By taking advantage of the correlation between the rf compression and the laser injection phase, the error caused by the jitter of the accelerating field in the gun is minimized and thus 10 fs time resolution is expected. Experimental demonstration at the Tsinghua Thomson scattering x-ray source with a time resolution better than 35 fs is reported in this paper. The experimental results are successfully used to obtain information on the possible cause of the jitter and the accompanying drifts.

DOI: 10.1103/PhysRevSTAB.17.032803 PACS numbers: 41.75.Ht, 29.27.-a

I. INTRODUCTION

Synchronization between the electron beam and the laser is crucial for the Thomson scattering (or inverse Compton scattering) x-ray source [1–3], the seeded x-ray free electron laser [4–6], and the MeV ultrafast electron diffractions [7–11]. The jitter between the electron beam and the laser pulse in these machines must generally be less than a subpicosecond to achieve stable x-ray pulse generation and sufficient time resolution in applications such as pump-probe experiments. Photocathode rf guns are commonly employed as the electron source in such facilities to generate a stable and bright electron beam because of their capacity to generate high brightness and a precise timed electron beam. A driving laser irradiates the cathode and generates the electron through the photoelectric effect. Modern techniques demonstrate precise control of two independent mode-locked oscillators with timing jitter at 10 fs or less [12]. Moreover, the driving laser of the photocathode gun and the TW scattering (or seeding, pump) laser come from a common oscillator. Hence, the fluctuation of the travel time of electron pulses mainly contributes to the timing jitter after the prompt generation of the pulses in the photocathode rf gun triggered by the driving laser and during the acceleration and transportation processes. The rf-to-laser jitter in the gun, the rf amplitude fluctuation in the gun and acceleration section, and the energy-dependent time of flight in the transport line contribute to the fluctuation. The rf-to-laser jitter in the photocathode rf gun is one of the dominant contributors. The characterization of this jitter and knowledge about its possible origins are important to compensate or remove the jitter for future stability improvements of the system.

In previous studies, the rf-to-laser jitter in the photocathode rf gun is measured by the method based on the photoelectron emission process [13–17] or by measuring the variation of time of flight related to the rf-to-laser jitter in the gun [13,18–20]. In the current work, we present a new beam-based method to measure the jitter in the photocathode rf gun. This method is based on the rf phase-related compression effect in the gun; such an effect is caused by the slippage of electron relative to the rf phase [21–26]. The rf-to-laser jitter in the photocathode rf gun is measured by analyzing the variation of the compression ratio of the beam. High time resolution is expected with this method since it is sensitive to the rf-to-laser jitter and insensitive to the other jitter sources such as the rf amplitude fluctuation in the gun, the rf phase and amplitude in the following acceleration sections. Analysis shows that the resolution is about 10 fs under normal machine parameters. Improving the resolution is limited by the jitter of the rf amplitude and the related measurement error of the compression ratio.

This method is successfully demonstrated at Tsinghua Thomson scattering x-ray source (TTX) [27]. TTX is the first dedicated hard x-ray source based on Thomson scattering in China. TTX aims to generate bright quasimonochromatic x-ray pulse ranging from 30 to 50 keV in the energy region. In previous experiments, the estimated arrival time jitter of the electron beam is about 0.5 ps. In

*dych@mail.tsinghua.edu.cn

TTX, the dominant contributions to the rf-to-laser jitter in the photocathode rf gun are fixed on the high voltage jitter of the modulator for shot-to-shot fluctuations and on the thermal drifts of the cooling water of the gun for slow fluctuations. A peak at 0.42 Hz, which is probably caused by the undersampling of the higher frequency of the power grid, is also observed.

In the present paper, we discuss the measurement techniques and their applications to characterize jitter performance. The rest of the paper is organized as follows. In Sec. II, the method is described and its time resolution is simulated and analyzed. In Sec. III, the experiment results at the TTX are presented and discussed. In Sec. IV, the conclusion is provided.

II. METHOD DESCRIPTION

A. Compression effect in the photocathode rf gun

The rf phase-related bunch compression in an rf gun has been reported and analyzed in previous works. It is shown as the sensitivity of ϕ_G, the asymptotic phase at the end of the gun, to variation in ϕ_0, the laser injection phase. Kim's theory described it in a simple mode [21]. Combining Kim's theory and simulation, Travier has shown that the ϕ_G is given in terms of the ϕ_0 as [25]

$$\phi_G = \phi_0 + \frac{1}{2\alpha \sin(\phi_0 + \frac{\pi}{6\sqrt{\alpha}})} + \frac{\pi}{15\alpha}, \tag{1}$$

where $\alpha = \frac{eE_0}{4\pi f mc}$ with e the electronic charge, m its mass, E_0 is the peak accelerating electric field, and f is the rf frequency. Then we may write the bunching ratio R, i.e. the ratio of the bunch length exit of the gun (σ_f) and the driven laser length (σ_i), as [23,24]

$$R = \frac{\sigma_f}{\sigma_i} = \frac{\partial \phi_G}{\partial \phi_0} = 1 - \frac{\cos(\phi_0 + \frac{\pi}{6\sqrt{\alpha}})}{2\alpha \sin(\phi_0 + \frac{\pi}{6\sqrt{\alpha}})}. \tag{2}$$

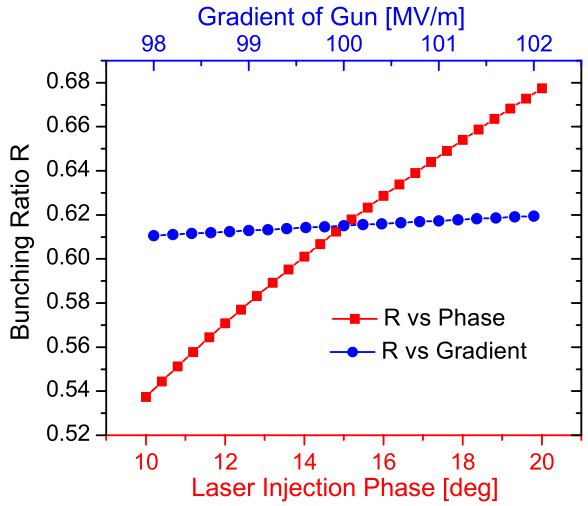

FIG. 1. Bunching ratio R versus laser injection phase and gun gradient. The rf frequency is 2856 MHz, and the gun gradient is 100 MV/m. The laser injection phase is fixed to 15 degrees for R versus gun gradient.

Figure 1 shows the bunching ratio R as a function of the laser injection phase and gun accelerating field given by Eq. (2) with a common photoinjector case, i.e. $f = 2856$ MHz, $E = 100$ MV/m. It clearly shows that the ratio R is quasilinear function of ϕ_0 in a relevant phase range. Therefore sensitivity of the bunching ratio to the laser injection phase can be employed to measure the rf-to-laser jitter in the photocathode rf gun. The bunching ratio versus the gun gradient is also shown in Fig. 1. Unlike the time of flight of the beam at the gun exit [23,26], there is slight sensitivity of the bunching ratio on the gun accelerating field variation, because the compression procedure (difference in the time of flight between the beam head and tail) mainly takes place during a short time interval immediately after photoemission adjacent to the cathode when the electrons are still nonrelativistic [26]. Further study shows that the bunching ratio is also slight sensitivity on the other jitter sources which may cause unwanted error during the measurement, such as the rf amplitude fluctuation in the gun, the rf phase and amplitude in the following acceleration sections. These mean that high time resolution may be achievable for rf-to-laser jitter measurement with this method we proposed in this paper.

A particles-in-cell (PIC) program instead of the theory analysis, GPT [28] (General Particle Tracer), is performed to precisely simulate the particles longitudinal motion to understand the compression procedure and its relationship to the jitter sources. The layout of the beam line in simulation is based on the injector of TTX and shown in Fig. 2. It is part of a common photoinjector. It mainly

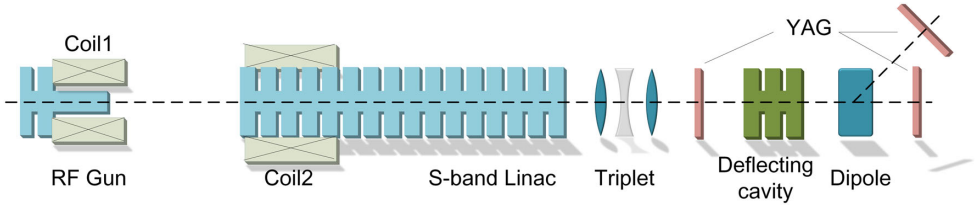

FIG. 2. Layout of beam line in simulation.

TABLE I. Beam line parameters used in simulations.

Parameter	Value	Units
Gun gradient	100	MV/m
Laser injection phase	15	degree
Laser pulse width (rms)	0.5	ps
Linac acceleration field	15	MV/m
Linac phase	Maximum acceleration	/
Solenoid after gun	0.22	T
Laser spot size(rms)	0.25	mm

includes a 1.6 cell BNL/KEK/SHI-type photocathode rf gun and a 3 m SLAC-type acceleration section located 1.5 m downstream of the cathode. The parameters used in simulations are listed in Table I. The parameters of the solenoids and laser spot size are not optimized since we mainly concern the beam's longitudinal dynamics. The space charge effect is not included in the simulation here and we will discuss it later.

Figure 3 shows the bunching ratio R versus the parameters which may affect the beam's longitudinal dynamics, i.e. the gun phase, gun peak field, linac acceleration field and linac phase. As shown in Fig. 3, the bunching ratio R is mainly influenced by the rf-to-laser jitter in the gun, 1 degree of rf-to-laser jitter in the gun leads to about 0.02 bunching factor jitter. The jitter of gun rf field amplitude slightly influences to R, 1% amplitude jitter will cause 4×10^{-4} jitter of R at laser injection phase $\phi_0 = 15^0$. The jitter of rf phase also has slightly effect to R with a coefficient 5.6×10^{-4}/degree, and the amplitude in the linac has much less effects to R. The relative time-of-flight (TOF) jitter versus these parameters is also shown in Fig. 3. Bunch compression and TOF are related. The variation of TOF caused by the jitter of laser injection phase $\Delta\phi_0$ can be expressed as $\Delta T_{\text{tof}} = (R-1)\Delta\phi_0$ [26]. The rf-to-laser jitter can also be measured by recording the variation of TOF with this relationship [13,18–20], but the resolution may be limited because the jitter of gun gradient also significantly leads to a variation of TOF, as shown in Fig. 3(b). The jitter of gun gradient leads to a variation of beam energy and then leads to a variation of TOF in the drift downstream the gun which approximately equals to $\frac{L}{c}\frac{\Delta\gamma}{\gamma^3}$. The influence of jitters in linac to TOF can be ignored since the beam is accelerated on the rf crest and boosted to high energy soon.

The space charge effect plays an important role in longitudinal dynamics. The Coulomb repulsion between the electrons always significantly lengthens the pulse

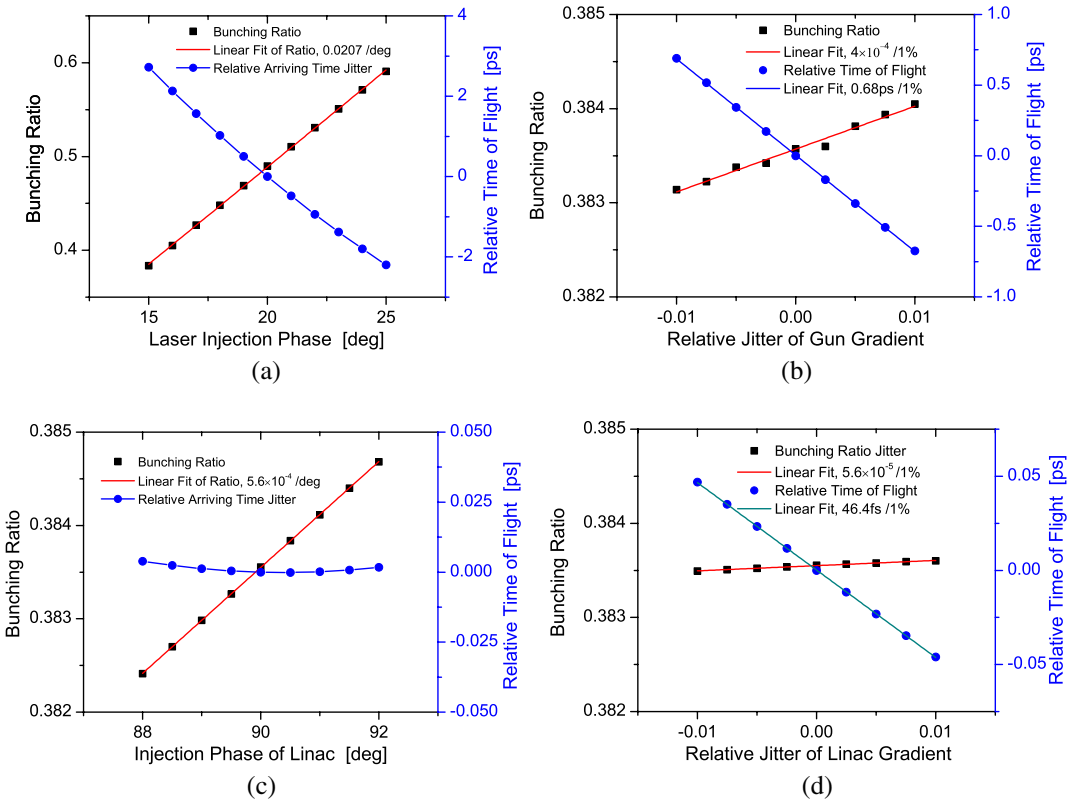

FIG. 3. PIC simulations of beam bunching ratio and relative time of flight at the linac exit versus (a) laser injection phase; (b) relative jitter of gun gradient with $E_{\text{Gun}} = 100$ MV/m; (c) injection phase of linac; (d) relative jitter of linac gradient with $E_{\text{acc}} = 15$ MV/m. No space charge effect is included in the simulations. Other parameters used in simulation are listed in Table I. References of TOF are subtracted to plot in the suitable y scale.

duration especially adjacent to the cathode when the electron is nonrelativistic. The repulsion depends on the charge density. Any jitter of the parameters which influence the charge density, such as the driving laser energy, laser pulse width, laser spot size on the cathode, may cause unwanted variation of bunching ratio. The rf-to-laser jitter in the gun and its related electron emission process will also cause the change of beam charge density. Figure 4 illustrates PIC simulation results with the space charge effect. Even the charge is as low as 1 pC, the strong relevant relations between the beam charge and the ratio R will cause unwanted measurement error and limit the measurement resolution. A low beam charge (or low beam intensity) aids in reducing the influence of the beam charge jitter. However, the poor signal-to-noise ratio may cause other unwanted measurement errors and limit the resolution.

A bunch train technique is helpful to exclude the influence of Coulomb repulsion. A pair of driving laser pulses with a distance of several picoseconds instead of a single-pulse driving laser is used to irradiate the cathode. Ratio R is calculated with the distance between the centers of the two pulses. The pair of driving laser pulses with fixed separation can be generated by an alpha-barium borate (a-BBO) crystal [29–31] or a beam splitter plate [32]. R versus beam charge jitter at different laser injection phases are simulated and compared with the cases in single pulse. The results are shown in Fig. 4. The charge of each pulse is 1 pC, and the separation between the two pulses is 5 ps. Although each pulse is still significantly expanded by Coulomb repulsion, the average center of the two pulses is slight sensitivity on the beam charge jitter because of the sufficient distance between the two pulses. For example, 3% beam charge jitter only causes about 9×10^{-5} variation of R, corresponding to about 4 fs resolution limitation. The effect of laser spot size jitter on the cathode is also simulated and shown in Fig. 5, the resolution limited by 5% laser spot size jitter is about 7 fs. Another advantage of the bunch train technique is that the result is independent of the longitudinal pulse shaping of each driving laser pulse, which may change during laser transmission.

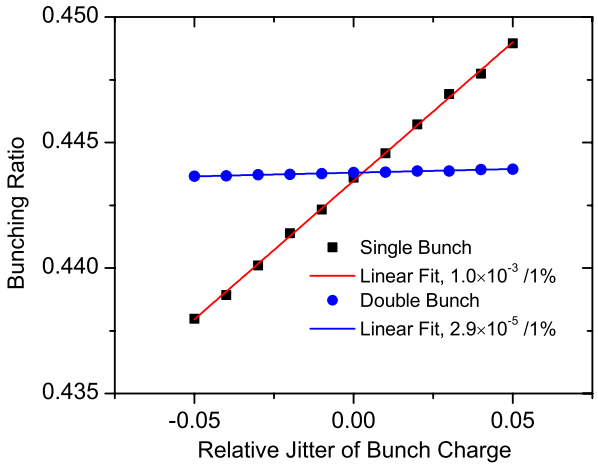

FIG. 4. Bunching ratio as a function of the bunch charge jitter by the PIC simulations with space charge effect. The total charge in simulation is 1 pC for single bunch and 2 pC for double pulses, respectively. The separation of the two driving laser pulses is 5 ps. Other parameters in simulation are listed in Table I.

B. Analysis of time resolution

High time resolution is expected with this method. The time resolution is mainly limited by the variation of R caused by other jitter sources and by the measurement. We assume no correlated jitter between the sources of jitter. Then we can write the fluctuation of R measured in the experiment as

$$\Delta R = \sqrt{(k_{\mathrm{Gun\_}p}\Delta\phi_{\mathrm{Gun}})^2 + (k_{\mathrm{Gun\_}E}\Delta E_{\mathrm{gun}})^2 + (k_Q\Delta Q)^2 + (k_{\mathrm{acc\_}p}\Delta\phi_{\mathrm{acc}})^2 + (k_{\mathrm{acc\_}E}\Delta E_{\mathrm{acc}})^2 + \cdots + (\Delta R_m)^2}, \quad (3)$$

where $\Delta\phi_{\mathrm{Gun\_}p}$, ΔE_{Gun}, Δ_Q, $\Delta\phi_{\mathrm{Acc}}$, ΔE_{acc} are the jitter of rf-to-laser in the gun, gun rf field amplitude, beam charge, linac acceleration phase and linac acceleration field, respectively, and k is the coefficient related the jitter source and ΔR. ΔR_m is the measurement error/resolution which depends on the employed technique. The first one at right is the variation caused by the rf-to-laser jitter in the gun which we want to measure. The rest of the parts are the deviations caused by other jitter sources and measurement error which limit the resolution of this method.

The contributions of the most important jitter sources are summarized in Table II. The coefficients can be determined by linear fitting with the simulation data, as shown in Figs. 3, 4, and 5. The resolution limited by the fluctuation of rf amplitude in the gun and linac, the rf phase in the linac and the beam charge is about 10 fs. The jitters of laser spot size and the linac acceleration phase contribute most of the limitation. The other jitters such as bunch charge, the rf amplitude in the gun and linac have relative less contribution.

From above calculation it is clear that one advantage of the method is to minimize the error caused by the fluctuation of rf amplitude in the gun. The error is less than 3 fs caused by 0.1% rf amplitude fluctuation, which is much smaller than by other methods. By the method mentioned in Refs. [13,16] based on the photoelectron emission process dominated by the Schottky effect and space charge effect, the jitter of gun rf amplitude will cause

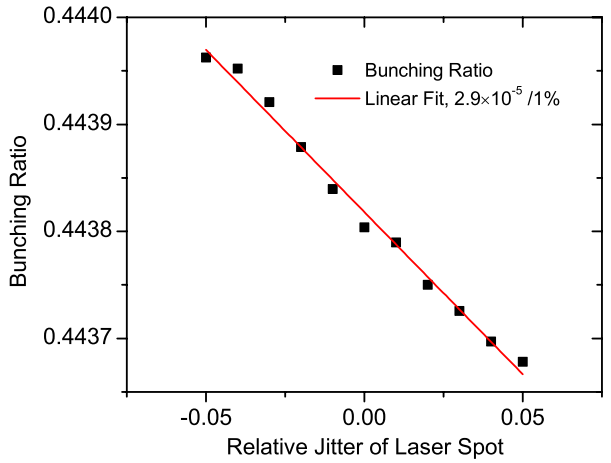

FIG. 5. The effects of the laser spot size jitter on the two pulses case with space charge effect.

variation of beam charge significantly. The estimated variation of charge caused by 0.1% jitter of gun rf amplitude approximately equals to that caused by several tens fs rf-to-laser jitter, thus the time resolution is limited to this value. The influence of the gun rf amplitude jitter is slight and negligible for the cathode that the photoelectron emission is weakly dependent of the gun gradient [15,17]. The rf amplitude jitter in the gun will also cause variation of time of flight. As shown in Fig. 3(b), 0.1% jitter of gun gradient will cause about 70 fs relative time of flight jitter. Thus, the time resolution of the method by measuring the jitter of time of flight led by the rf-to-laser jitter in the gun is limited to be about 70 fs$/(R-1) = -110$ fs.

The measurement error ΔR_m depends on the approach applied. Electro-optic technique [33–36], transverse deflecting cavity [37] can be employed to measure the separation of the electron pulses. Here we only analyze the case with a deflecting cavity, which is employed in our experiment in the following section. The measured separation of the two pulses on the beam profile monitor downstream the deflecting cavity is given as

$$d = L \cdot k \cdot s \cdot \frac{eV_{def}\cos\phi_{\mathrm{def}}}{W}, \tag{4}$$

where L is the drift length between the deflecting cavity and the beam profile monitor, k is the rf wave number, V_{def} is the maximum deflecting voltage, W is beam energy, s is the separation of the two pulses, ϕ_{def} is the phase when the particle pass the cavity and $\phi_{\mathrm{def}} \approx 0$ in the measurement.

The measured error of d can be written as

$$\Delta d = \frac{\partial d}{\partial V_{\mathrm{def}}} \cdot \Delta V_{\mathrm{def}} + \frac{\partial d}{\partial W} \cdot \Delta W + \frac{\partial d}{\partial \phi_{\mathrm{def}}} \cdot \Delta\phi_{\mathrm{def}}. \tag{5}$$

If there is no correlation between the parameters, the relative measured error is

$$\Delta R_m = \frac{\Delta d}{d} = \sqrt{\left(\frac{\Delta V_{\mathrm{def}}}{V_{\mathrm{def}}}\right)^2 + \left(\frac{\Delta W}{W}\right)^2 + (\tan\phi_{\mathrm{def}}\Delta\phi_{\mathrm{def}})^2}. \tag{6}$$

0.1% jitter of deflecting voltage or beam energy will lead 10^{-3} variation of R, corresponding to about 50 fs error to rf-to-laser jitter measurement with the coefficients listed in Table II. This error can be removed by normalization. This requires measuring both beam energy and deflecting voltage shot-by-shot simultaneously. Increasing the stability of these parameters can help in achieving high measurement accuracy. Modern technology can increase the stability of rf amplitude and beam energy in about one order to 10^{-4} [38]; thus, a time resolution about 10 fs may be achievable. In some specific beam line layouts, the beam energy and deflecting voltage are correlated and the error can be dramatically reduced. For example, the photocathode rf gun, linac, and deflecting cavity at the TTX are supplied by one klystron; their influences on jitter measurement are fully canceled. The error caused by the phase jitter in deflecting cavity can be ignored while the beam is deflected at zero phase ($\phi_{\mathrm{def}} = 0$), i.e. the error caused by 1 degree deflecting phase jitter is less than 7 fs.

Complete tracking simulations with the TTX beam line layout (Fig. 2) that include all the jitters simultaneously are performed to obtain a statistically significant evaluation of the time resolution. By randomly Gaussian sampling each parameter within a tolerance range listed in Table III, 300

TABLE II. Summarization of the error caused by the most important jitter source; the assumed stability in the calculation is well within the reach of present rf technology.

Jitter source	Coefficient to ΔR	Jitter	ΔR	Contribution to time error (fs)
Laser injection phase	0.0207/degree	To be measured		
Gun rf amplitude	4.5×10^{-4}/1%	0.1%	4.5×10^{-5}	< 3
Bunch charge	2.9×10^{-5}/1%	3%	9×10^{-5}	4
Laser spot size	2.9×10^{-5}/1%	5%	1.45×10^{-4}	7
Linac phase	5.6×10^{-4}/degree	0.3°	1.7×10^{-4}	8
Linac phase	1×10^{-5}/1%	0.1%	1×10^{-6}	< 1
Total				< 11.5

TABLE III. Variations of the parameters in complete tracking simulations.

Parameters	rms variation	Units
Laser injection phase	0.3	degree @ 2856 MHz
Gun rf amplitude	0.1%	···
Linac rf amplitude	0.1%	···
Deflecting cavity rf amplitude	0.1%	···
Beam charge	3%	···
Linac phase	0.3	degree @ 2856 MHz
Laser spot size	5%	···
Deflecting cavity phase	0.3	degree @ 2856 MHz

cases are tracked with GPT. All jitter sources discussed above are included in the simulation. Other jitters, such as the solenoid current, the separation of the driving laser pulses, and the laser pulse width, are neglected in the simulations because of their high stability or negligible impact on the bunching ratio. The jitter of rf amplitude in gun, linac and deflecting cavity are the same since they are powered by one klystron. The simulated bunching ratio versus laser injection phase jitter is shown in Fig. 6. The residual uncorrelated noise of bunching ratio is 2.8×10^{-4} which corresponds to ~14 fs error for rf-to-laser jitter measurement. This value is a little larger than that in Table II, since the jitters of rf-to-laser and rf amplitude in the gun will also cause the jitter of the linac acceleration phase and thus induce the fluctuation of bunching ratio which is not included in Table II.

III. EXPERIMENT AT TTX

This method is demonstrated at TTX to determine the possible origins of the timing jitter between the driving laser and the gun rf phase. The layout of the beam line is

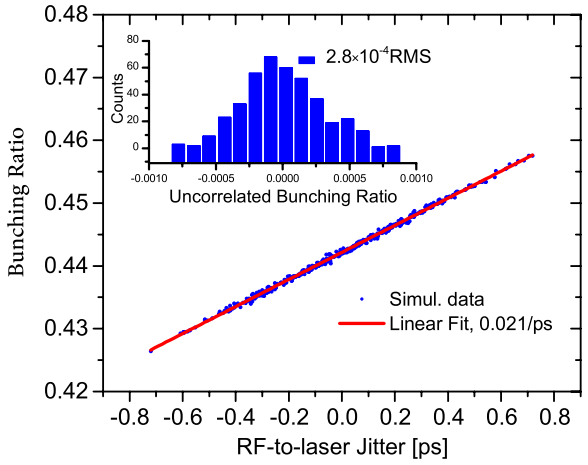

FIG. 6. Correlation between the rf-to-laser jitter in the gun and the bunching ratio in the simulation. A residual uncorrelated bunching ratio is about 2.8×10^{-4} rms, corresponding to ~14 fs time resolution limitation for the rf-to-laser jitter measurement.

TABLE IV. Jitter of experiment parameters and the simulated coefficients to ΔR.

Parameters	Coefficient (simulated)	rms variation
Laser injection phase	0.0265/degree	To be measured
Gun rf amplitude	$2.7 \times 10^{-3}/1\%$	$< 0.1\%$
Beam charge	$4 \times 10^{-5}/1\%$	$< 2.5\%$
Linac phase	$8.5 \times 10^{-4}/1\%$	< 0.5 ps (estimated)
Laser spot size	$4 \times 10^{-5}/1\%$	···

shown in Fig. 2. A modified version of the BNL/KEK/SHI type 1.6 cell photocathode rf gun [39,40] and a 3 m SLAC-type traveling wave accelerating section are used to generate ultrashort, high charge, and low-emittance electron pulses. A deflecting cavity is employed to measure the longitudinal distribution of the beam and the relative compressor ratio [41]. The gun, acceleration section, and deflecting cavity are powered by the same klystron. The rf amplitude and phase in the gun, acceleration section and the deflecting cavity can be adjusted separately with phase shifters and attenuations. A Ti:sapphire laser system is used to generate both the TW ultrashort infrared (IR) scattering laser and the ultraviolet driving laser for the photocathode rf gun. A pair of driving laser pulses with a ~12.67 ps separation is generated by a 16 mm thick alpha-BBO crystal [31]. The laser spot size on the cathode is 0.25 mm rms. The total beam charge is reduced to ~1 pC with ~2.5% rms stability in the experiments. The gun gradient is reduced to about 70 MV/m with a repetition of ~5 Hz to avoid rf arc damage. The coefficients of ΔR to the jitter sources with experimental parameters are simulated by GPT and listed in Table IV.

The ratio R is calculated by the measured longitudinal distribution of the beam with the deflecting cavity. The typical measured beam profile and projected distribution after the deflecting cavity are shown in Fig. 7. The weak

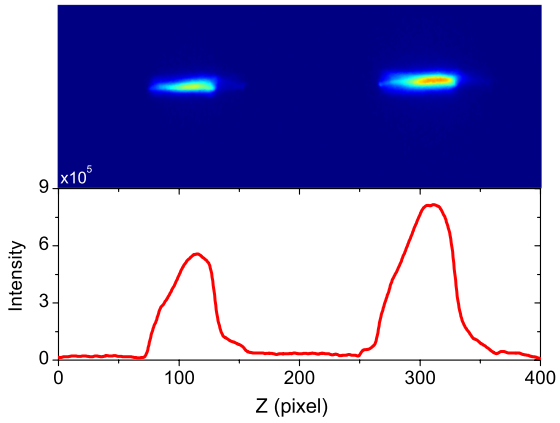

FIG. 7. Typical measured y-z distribution of the beam with a pair of driving laser pulses measured using the beam profile monitor system when the deflecting cavity is on. The centroid of each pulse is found through bi-Gauss curve fitting.

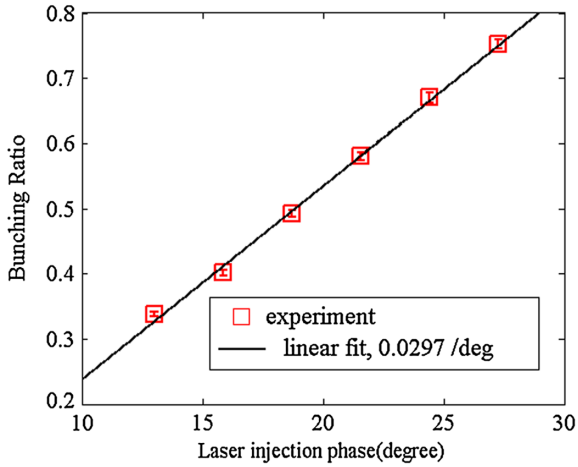

FIG. 8. Calibration curve of the rf-to-laser timing jitter in the gun. Each data point on the graph represents the average of 20 shots and the vertical error bar indicates the rms spread in the gathered data. The error bar is hidden within the marker size. The relative delay between the rf phase in the gun and the driving laser is moved with an rf phase shifter to regulate the coefficient between the phase jitter and the R variation.

intensity pulse is launched at a low laser injection phase. Bi-Gauss fitting is applied to the projected distribution to find the center of each pulse and the distance between these pulses with high accuracy. Ratio R is then obtained with this measured value divided by the distance between the driving laser pulses.

Measuring the timing jitter requires system calibration. The coefficient between the launched phase and ratio R is calibrated by changing the timing between the driving laser and the gun phase (with a phase shifter on the waveguide to the gun) and by monitoring the related ratio R. Figure 8 shows the measured results of R as a function of the launched gun phase. Each data point on the graph represents the average of 20 shots and the vertical error bar indicates the rms spread in the gathered data. Determined by linear fitting, the coefficient is 0.0297/degree. It is ~10% larger than the simulation result which may be caused by the higher gun accelerating field in the simulation or the shorter laser pulses separation used in the coefficient calculation. This value indicates that a 0.01 variation in ratio R corresponds to 330 fs timing jitter of rf -to laser in the gun. To eliminate the possible distortion of the calibration by time drifts, this calibration is repeated; the same results are achieved.

A typical measurement result with 2700 shots (~9 min) is shown in Fig. 9. The histogram of the total signal is shown in Fig. 9(b). The measured rf-to-laser jitter in the photocathode rf gun is about 410 fs rms. A noticeable slow drift is observed during the measurement. By subtracting the low frequency (< 1 Hz) drifts, the jitter is reduced to

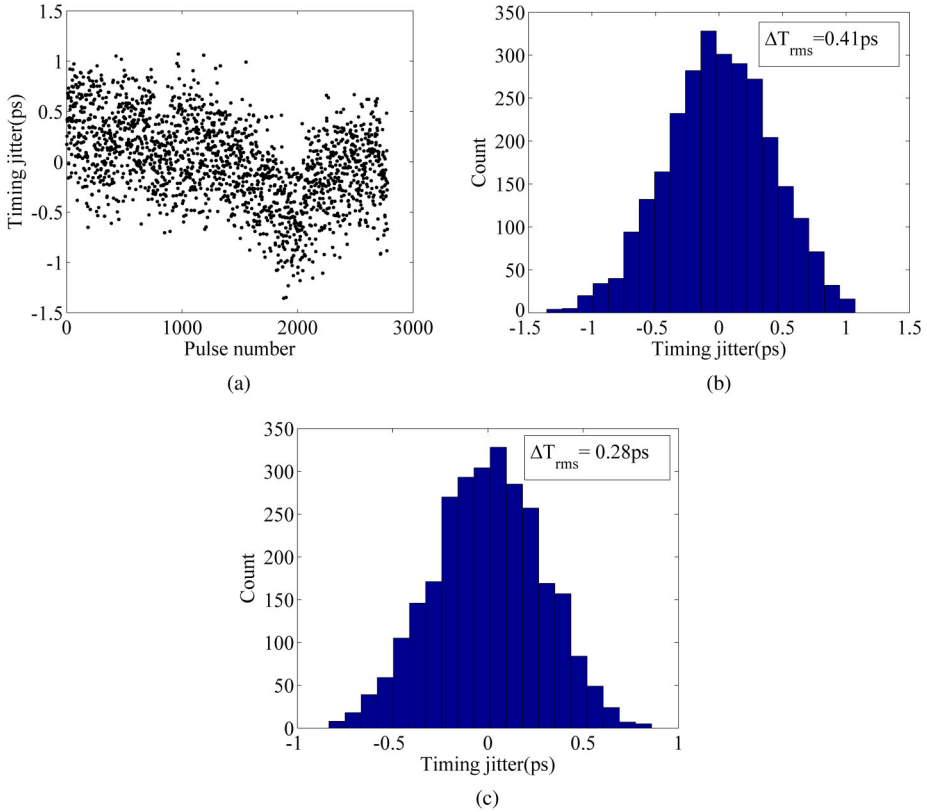

FIG. 9. (a) A 9 min (2700 shot) measurement of the relative delay between the driving laser and the rf phase in the gun. (b) Histogram of the total signal and (c) the removal of the slow drift.

~280 fs rms. The histogram after the removal of the low frequency drifts is shown in Fig. 9(c).

A frequency analysis of the signal is carried out to determine the possible origins of the jitter, as shown in Fig. 10. Two featuring peaks exist: a peak at around 0.42 Hz and a peak that corresponds to slow drifts. The leading cause of the slow drifts should be the temperature drift of the cooling water of the gun which is also observed in other laboratories [17]. The temperature variation of the cooling water is ~0.1 degree Celsius peak to peak, which theoretically causes ~1.6 ps gun rf phase shift with a gun Q value of ~10000. The cycle time of the drifts is also similar (several minutes). Thermal drifts in the cables that guide the rf signal from the rf source to the klystron and laser room also cause slow drifts, but the cycle time (several hours) is much longer than that measured in this experiment. The origin of the 0.42 Hz peak is unclear. One possibility is related to an undersampled power grid frequency. The beat frequency of the trigger repetition (4.958 Hz) and the power grid frequency (50 Hz) are both 0.42 Hz, which is very close to the peak observed in the experiment. Similar results have also been reported [42]. The total contribution of the slow drifts is about 300 fs. The residual shot-to-shot jitter, except at the low frequency drifts, is about 280 fs. The most dominant contributor is the jitter of the high voltage applied to the klystron (Toshiba E3730 A). The measured rms jitter of the high voltage of the modulator is 0.06%, which results in a 250 fs rf phase jitter on the klystron output. The synchronization error between the rf signal and the laser oscillator (< 100 fs) [43] also contributes to the shot-to-shot jitter. However, this contribution is limited because it is about 3 times smaller than that caused by a high voltage jitter.

The time resolution in this experiment is analyzed as follows. The beam charge jitter is about 2.5% rms. With the simulated coefficient of bunching ratio and beam charge jitter, $4 \times 10^{-5}/1\%$, one finds resolution smaller than 5 fs. The laser spot size fluctuation can be eliminated because the laser spot is cut by an iris and an imaging relay system is employed to transport it to the cathode. The measured rf amplitude jitter in the gun is less than 0.1%; it is equivalent to a resolution limitation about 10 fs. The linac accelerating phase jitter which combines the rf phase jitter from the klystron and the beam time of flight jitter is estimated to be less than 0.5 degree, this corresponds to 4.3×10^{-4} bunching ratio fluctuation, or about 15 fs rms resolution limitation. Because the gun, the accelerating section, and the deflecting cavity are powered by one klystron, the measurement error caused by the rf amplitude fluctuation and related beam energy jitter can be counteracted and ignored. The time resolution is mainly limited by the resolution of the distance measurement of the two pulses and the rf amplitude jitter in the gun. Limited by the rf power fed to the deflecting cavity and the imaging system used in the beam profile monitor system, the typical separation of the two pulses on CCD is about 120 pixels (Fig. 7). Assuming that the curve fitting error to fix the position of the two pulses is 0.1 pixels, the relative error of the measurement is estimated to be 8.3×10^{-4}, which corresponds to a jitter measurement error of about 28 fs. Assuming all error sources are uncorrelated, the time resolution of the experiment should be better than 35 fs.

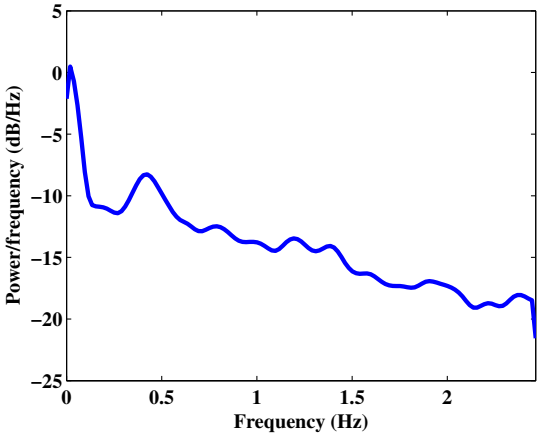

FIG. 10. Power spectral density of the data shown in Fig. 9. The spectrum is obtained using the Welch method and the function psd in the MATLAB software.

IV. CONCLUSION

A high time resolution method based on the laser injection phase related compression in the photocathode rf gun is proposed. Simulations show that this method is sensitivity on the rf-to-laser jitter in the gun and slight sensitivity on other jitter sources in the system and then inherence high time resolution is expected. A time resolution of ~10 fs is achievable with the normal accelerator parameters.

This method is successfully demonstrated at TTX and is used to determine the possible origins of jitter. The estimated time resolution of the measurement is better than 35 fs. The measured jitter (410 fs) has two parts: low frequency drifts (~300 fs) and shot-to-shot jitter (~280 fs). The analysis of the spectrum of the jitter shows a clear peak at 0.42 Hz, which is probably caused by the undersampling of the higher frequency of the power grid. The thermal drift of the cooling water of the gun may be the main cause of the low frequency drifts. The jitter of the high voltage applied to the klystron is the most dominant cause of the shot-to-shot fluctuation. Based on the measurement, a low-level rf (LLRF) system is suggested to feed back the slow drifts. A highly stable modulator is required to achieve a low shot-to-shot timing jitter. A feed-forward control of high voltage jitter of the modulator in LLRF is also suggested in further upgrades.

ACKNOWLEDGMENTS

This work is supported by the National Natural Science Foundation of China (Grants No. 11127507 and No. 11375097) and by the National Basic Research Program of China (973 Program) (Grant No. 2011CB808302).

[1] K.-J. Kim, S. Chattopadhyay, and C.V. Shank, Nucl. Instrum. Methods Phys. Res., Sect. A **341**, 351 (1994).
[2] A. Ting *et al.*, Nucl. Instrum. Methods Phys. Res., Sect. A **375**, ABS68 (1996).
[3] R. W. Schoenlein, W. P. Leemans, A. H. Chin, P. Volfbeyn, T. E. Glover, P. Balling, M. Zolotorev, K.-J. Kim, S. Chattopadhyay, and C. V. Shank, Science **274**, 236 (1996).
[4] I. Ben-Zvi, L. F. Di Mauro, S. Krinsky, M. G. White, and L. H. Yu, Nucl. Instrum. Methods Phys. Res., Sect. A **304**, 181 (1991).
[5] L.-h. Yu and I. Ben-zvi, Nucl. Instrum. Methods Phys. Res., Sect. A **393**, 96 (1997).
[6] L.-h.Yu *et al.* Phys. Rev. Lett. **91**, 074801 (2003).
[7] X. J. Wang, D. Xiang, T. K. Kim, and H. Ihee, *J. Korean Phys. Soc.* ***48****, 390 (2006)*.
[8] J. B. Hastings, F. M. Rudakov, D. H. Dowell, J. F. Schmerge, J. D. Cardoza, J. M. Castro, S. M. Gierman, H. Loos, and P. M. Weber, Appl. Phys. Lett. **89**, 184109 (2006).
[9] P. Musumeci, J. T. Moody, and C. M. Scoby, Ultramicroscopy **108**, 1450 (2008).
[10] R. K. Li *et al.*, Rev. Sci. Instrum. **81**, 036110 (2010).
[11] R. K. Li, C. Tang, Y. Du, W. Huang, Q. Du, J. Shi, L. Yan, and X. Wang, Rev. Sci. Instrum. **80**, 083303 (2009).
[12] J. Kim, J. A. Cox, J. Chen, and F. X. Kärtner, Nat. Photonics **2**, 733 (2008).
[13] H. Qian *et al.*, in *Proceedings of the 23rd Particle Accelerator Conference, Vancouver, Canada, 2009* (IEEE, Piscataway, NJ, 2009), p. TH6REP101.
[14] X. J. Wang *et al.*, in *Proceedings of the 19th International Linear Accelerators Conference, Chicago, Illinois, 1998* (NTIS, Springfield, VA, 1998), p. 866.
[15] M. Krasilnikov *et al.*, in *Proceedings of the 14th Beam Instrumentation Workshop, Santa Fe, New Mexico* (LANL, Los Alamos, 2010).
[16] M. Csatari Divall, M. Kaiser, S. Hunziker, C. Vicario, B. Beutner, T. Schietinger, M. Lüthi, M. Pedrozzi, and C. P. Hauri, Nucl. Instrum. Methods Phys. Res., Sect. A **735**, 471 (2014).
[17] H. Schlarb *et al.*, in *Proceedings of the 10th European Particle Accelerator Conference, Edinburgh, Scotland, 2006* (EPS-AG, Edinburgh, Scotland, 2006), p. TUPCH025.
[18] M. Kristin Bock, Ph.D. thesis, DESY, 2012.
[19] V. Arsov *et al.*, in *Proceedings of the 11th European Particle Accelerator Conference, Genoa, 2008* (EPS-AG, Genoa, Italy, 2008), p. THPC152.
[20] A. Gallo *et al.*, in *Proceedings of the 22nd Particle Accelerator Conference, Albuquerque, New Mexico* (IEEE, New York, 2007).
[21] K. J. Kim, Nucl. Instrum. Methods Phys. Res., Sect. A **275**, 201 (1989).
[22] C. Travier, Nucl. Instrum. Methods Phys. Res., Sect. A **340**, 26 (1994).
[23] P. G. O'Shea, in *Proceedings of the Particle Accelerator Conference, Dallas, TX, 1995* (IEEE, New York, 1995), p. 970.
[24] E. Ralph Colby, Ph.D. thesis, University of California, Los Angeles, 1997.
[25] X. J. Wang, X. Qiu, and I. Ben-Zvi, Phys. Rev. E **54**, R3121 (1996).
[26] R.-k. Li and C. Tang, Nucl. Instrum. Methods Phys. Res., Sect. A **605**, 243 (2009).
[27] Y. Du, L. Yan, J. Hua, Q. Du, Z. Zhang, R. Li, H. Qian, W. Huang, H. Chen, and C. Tang, Rev. Sci. Instrum. **84**, 053301 (2013).
[28] GPT—A simulation Tool for the Design of Accelerators and Beam Lines, http://www.pulsar.nl/gpt.
[29] H. Tomizawa, H. Dewa, H. Hanaki, and F. Matsui, Quantum Electron. **37**, 697 (2007).
[30] A. K. Sharma, T. Tsang, and T. Rao, Phys. Rev. ST Accel. Beams **12**, 033501 (2009).
[31] L.-X. Yan, J.-F. Hua, Y.-C. Du, Y.-F. Huang, Y. You, D. Wang, W.-H. Huang, and C.-X. Tang, J. Plasma Phys. **78**, 429 (2012).
[32] C. W. Siders, J. L. W. Siders, A. J. Taylor, S.-G. Park, and A. M. Weiner, Appl. Opt. **37**, 5302 (1998).
[33] B. Steffen *et al.*, Phys. Rev. ST Accel. Beams **12**, 032802 (2009).
[34] R. Pompili *et al.*, Nucl. Instrum. Methods Phys. Res., Sect. A **740**, 216 (2014).
[35] C. M. Scoby, P. Musumeci, J. T. Moody, and M. S. Gutierrez, Phys. Rev. ST Accel. Beams **13**, 022801 (2010).
[36] F. Müller, P. Peier, V. Schlott, B. Steffen, T. Feurer, and P. Kuske, Phys. Rev. ST Accel. Beams **15**, 070701 (2012).
[37] X. J. Wang, T. Srinivasan Rao, K. Batchelor, I. Ben-Zvi, and J. Fischer, Nucl. Instrum. Methods Phys. Res., Sect. A **356**, 159 (1995).
[38] T. Asaka *et al.*, in *Proceedings of the International Particle Accelerator Conference, Kyoto, Japan* (ICR, Kyoto, 2010), p. Tupe025.
[39] H. Qian, C. Tang, S. Zheng, D. Tong, H. Chen, W. Huang, and X. Guan, Nucl. Instrum. Methods Phys. Res., Sect. A **597**, 121 (2008).
[40] H. Qian *et al.*, in *Proceedings of the 34th International Free Electron Laser Conference, Nara, 2012* (Spring-8 and Kyoto University, Nara, Japan, 2012), p. MOPD55.
[41] S. Jia-Ru, C. Huai-Bi, T. Chuan-Xiang, H. Wen-Hui, D. Ying-Chao, Z. Shu-Xin, and R. Li, Chin. Phys. C **33**, S161 (2009).
[42] N. Čutić, C. Erny, F. Lindau, and S. Werin, Nucl. Instrum. Methods Phys. Res., Sect. A **626–627**, 16 (2011).
[43] Q. Du, Y. Du, L. Yan, W. Huang, J. Li, and C. Tang, Nucl. Instrum. Methods Phys. Res., Sect. A **637**, S137 (2011).